24th COBEM - 2017

24th ABCM International Congress of Mechanical Engineering
December 3-8, 2017, Curitiba, PR, Brazil

COBEM-2017-0946
INVESTIGATION OF THE HIGH ENERGY MODE BRANCH IN FLEXIBLE CYLINDERS VIV: A NOVEL RECURSIVE EXPERIMENTAL ANALYSIS METHODOLOGY

Wagner Antonio Defensor Filho

Celso Pupo Pesce

Guilherme Rosa Franzini

Offshore Mechanics Laboratory - Escola Politécnica, University of São Paulo, São Paulo, SP, Brazil
wadfilho@usp.br ; ceppesce@usp.br ; gfranzini@usp.br

Abstract. *An experimental investigation was conducted at a circulating water channel on the "high speed mode response branch", firstly revealed in the works by Fujarra et al 2001, from experiments with cantilevered flexible cylinders with orthotropic bending stiffnesses. Such a branch, herein called 'high energy mode branch' HEMB, is characterized by oscillation amplitudes of order of one diameter, in a range of reduced velocities much beyond the usual VIV lock-in peak. The present campaign systematically addresses the effect of the natural frequency ratio, f_{x1}/f_{y1}, on the HEMB. A response branch chart obtained as a function of reduced velocity and parameterized according to the frequency ratio is the ultimate focus of this investigation. The present paper describes the experimental methodology, including a novel experimental analysis procedure based on a recursive application of the Hilbert-Huang Transform. Preliminary experimental results are shown.*

Keywords: *Vortex induced vibrations; High Energy Mode Branch; Hilbert-Huang Transform; Empirical Mode Decomposition; experimental analysis methodology; flexible cylinders; fluid-structure interactions.*

1. INTRODUCTION

This work investigates further a vortex-induced vibration (VIV) 'high speed mode branch' in cantilevered flexible cylinders, discovered experimentally by Fujarra, *et al.*, 2001; see also Fujarra (2002). That work studied a flexible cylinder with orthotropic bending stiffness in a circulating water flume, such that the ratio between the first natural frequencies in the cross-wise and in the in-line directions to the flow was set very close to four (f_{x1}/f_{y1} = 4.08). Those experiments exhibited a new response branch, of large amplitude and high frequency, herein after renamed "High Energy Mode Branch" (HEMB), (see Fig. 1 – left), which took place in a wide range of reduced velocities, $12 \leq U^* \leq 22$, ($U^* = U/f_1D$). Such a HEMB was triggered by disturbing the steady VIV response, either structurally or by an upstream wake perturbation, and revealed a stable dynamic attractor in decreasing flow speeds. Previously in, Pesce & Fujarra (2000), (see also Pesce & Fujarra (2005)), a similar but much shorter HEMB had been found in a towing tank cantilevered flexible cylinder experiment, appearing just after the lock-in peak, and coexisting with the usual lower response branch (see Fig.1 - right). That shorter and stable HEMB was also excited in slightly decreasing reduced velocities, possibly triggered by the towing carriage vibrations. In that case, however, f_{x1}/f_{y1}=1.0.

To investigate this interesting flow-induced vibration phenomenon (the appearance of the HEMB) and aiming at understanding the causes and driving mechanisms of such dynamic behavior, a systematic experimental investigation was planned and carried out at NDF-USP water channel; see Assi (2005) for details on the experimental facility. The influence of the parameter, f_{x1}/f_{y1}, on the HEMB has been under investigation. In the present paper, the experimental planning and set up, including a non-conventional optical tracking system, as well as a novel experimental analysis methodology are presented and discussed, together with some preliminary results concerning one of the cylinders.

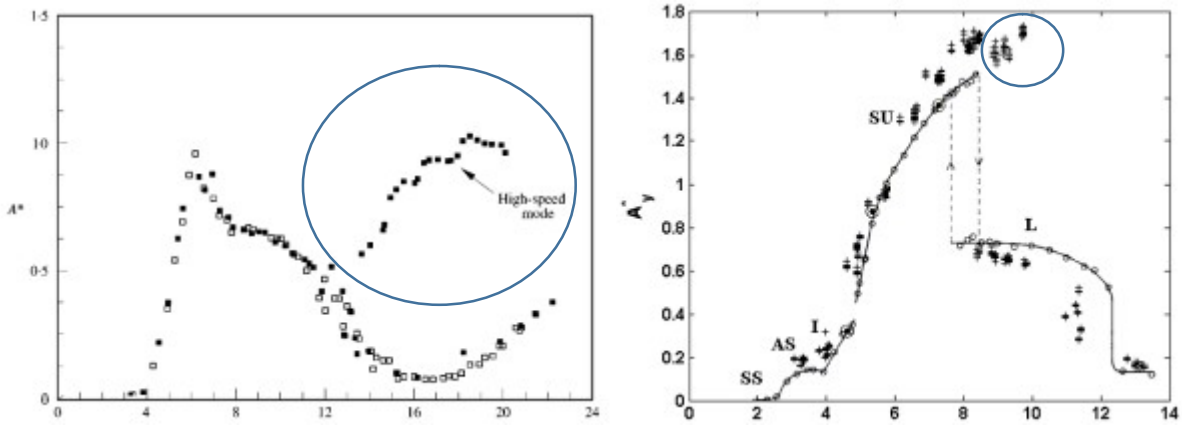

Figure 1. Crosswise dimensionless amplitude, $A^*=A_y/D$ as function of reduced velocity, $U^*=U/f_{y1}D$. Left: Emphasis on the long branch of response at higher reduced velocities, Fujarra *et al* (2001), Fujarra A. L. (2002); Right: Emphasis on the short branch of response, at $9<U^*<10$, Pesce and Fujarra (2005), after Pesce and Fujarra (2000) and Fujarra A. L. (1997).

2. DESIGN AND CONSTRUCTION OF THE FLEXIBLE CYLINDERS

A special design for the flexible cylinders with orthotropic bending stiffness has been applied. The concept is based on Fujarra, *et al.*, 2001; see also Fujarra (2002). The flexible cylinders are composed by polymeric cylinders molded over aluminum flat bars (strips), having cross sections of distinct aspect ratios. The structural design was based on FEM analysis, using Abaqus® code and on analytical formulations using Matlab, assuming perfect adhesion and linear elastic behavior.

To conform with the water channel characteristics, the models were designed as L=400mm long cantilevers with diameter D=10mm. The width/thickness aluminum strip ratio, t/b, controls the natural frequencies ratio. Four distinct natural frequencies ratio (in still water) were chosen: f_{x1}/f_{y1} = 1:1; 2:1; 3:1; 4:1. For that, four aspect ratios were taken: "2mm x 2mm", "2mm x 1mm", "3mm x 1mm" and "4mm x 1mm". The isotropic ratio model, f_{x1}/f_{y1} = 1:1, uses a 2mm x 2mm strip due to manufacturing difficulties on making 1mm width cuts. To calculate the natural frequencies in still water, the added mass coefficient was taken C_a =1,17, after Pesce and Fujarra (2000); see also Salles & Pesce (2017), so that the added mass is m_a = 36.757g. The mass ratio, $m^* = m/m_d$, take the values: 1.182; 1.141; 1.161; 1.181, where m_d is the displaced mass of fluid.

The strips material is aluminum and the polymeric cylindrical bodies were made by casting a soft resin commercially available. Initially, adopted nominal values were used for the materials mechanical properties, furtherly corrected by their respective as-built values. The as-built corrections were applied to the aluminum Young Modulus and to the polymeric resin density and Young Modulus.

The construction was made for a vertical assemblage, with the strip width aligned longitudinally (x axis) and the strip thickness aligned transversally to the flow (y axis). Figure 2 and 3 show, respectively, a view of the FEM models and the theoretical natural frequency ratios as function of the aluminum strip width.

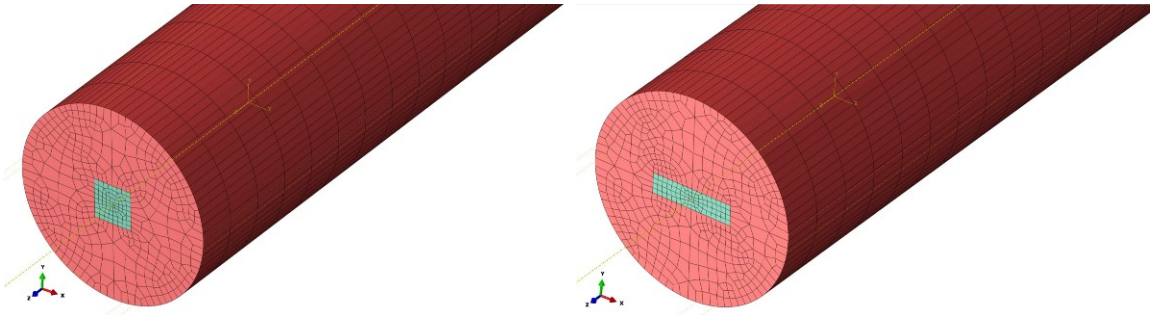

Figure 2. FEM model typical layout. Metallic strips in green. Left: 2mm x 2mm metallic strip; Right: 4mm x 1mm metallic strip; Higher stiffness in x direction (in-line with the stream).

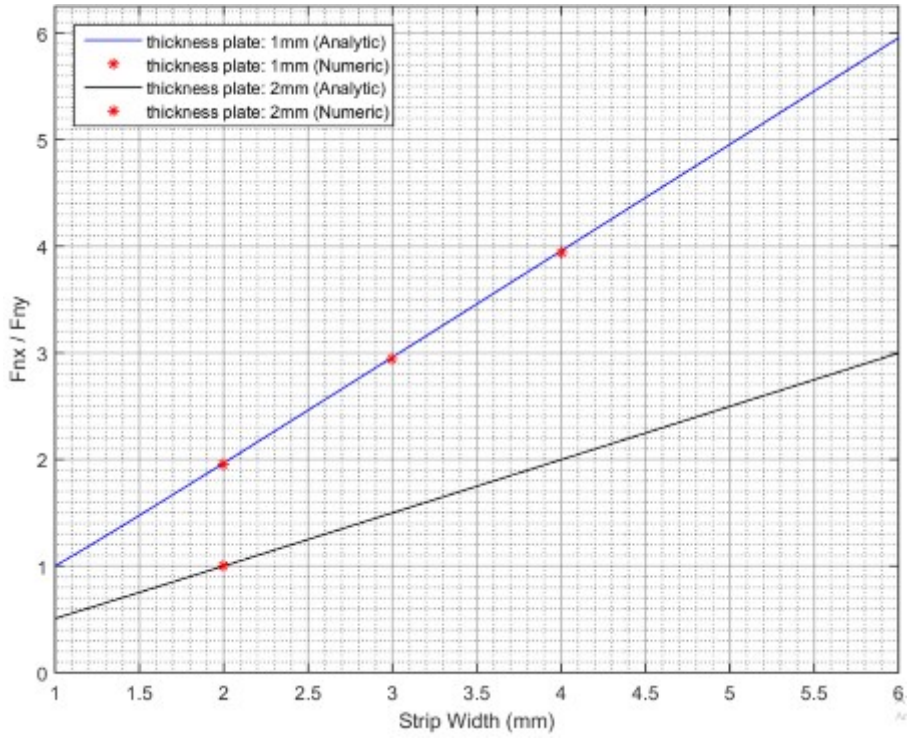

Figure 3. Comparison between analytical and numerical frequencies ratio. Red dots from numerical models.

After machining and hand finishing, an injecting process into a bipartite brass cast made the union between the aluminum strips and the polymeric cylindrical bodies. The strips were accommodated in a vertical position, aligned by 3D printed guides fixed at the cast top and bottom. The cantilever anchor was also 3D printed. The total length of the cylinder is 450mm. A 50mm long segment of the cylinder is then rigidly fixed into the anchor, such that the resulting free span is 400mm long, Fig. 4.

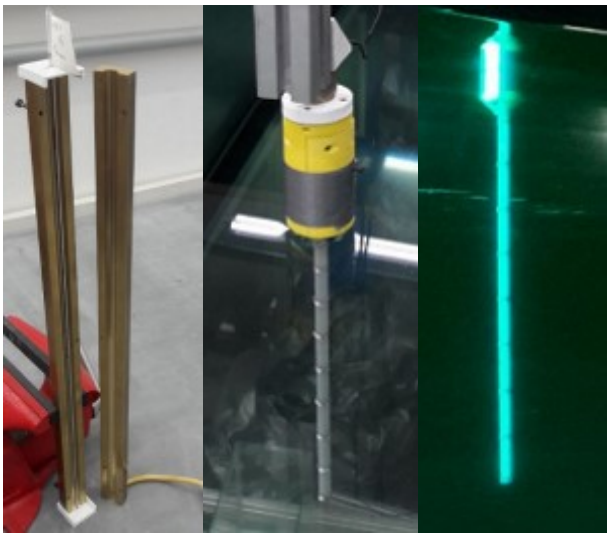

Figure 4. Left: Bipartite brass cast with a strip vertically positioned inside. Center: Anchor (yellow device) and flexible cantilevered cylinder positioned at the water channel, with reflective targets. Right: Whole set under the optical tracking system's light.

3. EXPERIMENTAL SET UP AND PROCEDURES

The experiments took place at NDF circulating water channel, located at Escola Politécnica, University of São Paulo. Figure 5 shows illustrative pictures of the experimental set up at NDF circulating water channel. Two underwater

Qualisys® system cameras, were positioned downstream the section at which the flexible cylinder models were assembled. Data acquisition occurred simultaneously with Labview® and Qualisys Track Manager® systems.

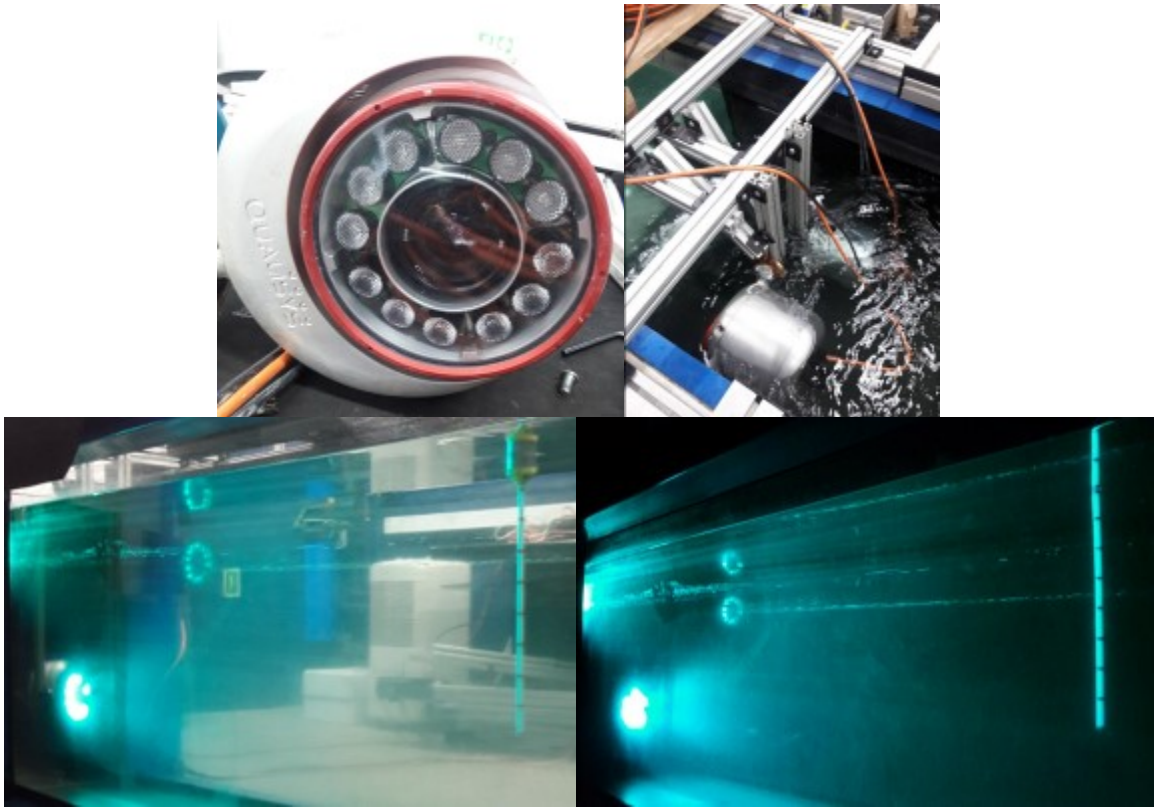

Figure 5. Top Left: Qualisys Track Manager® underwater camera; Top Right: Cameras assembling inside the circulating water channel at NDF; Bottom Left and Right: full experimental assembling positioned inside circulating water channel.

Labview® controlled the water channel flow speed and acquired the 6 DOF load cell information, placed at the top of the model (see Franzini, *et al*., 2015, 2016). Qualisys Track Manager® is an optical tracking system, which operates with underwater cameras and is capable to acquire the displacements of distinct cross sections directly, by tracking reflective tapes attached along the cylinder. This system presents advantages when compared to the classical strain-gage instrumentation, as is noninvasive (wireless) and permits the direct measurement of displacements. Its accuracy is of order of 0.05mm; see Salles and Pesce (2017) and has been already used in the NDF channel; see Franzini *et al* (2015).

The first experimental step is the calibration of the Qualysis® system. This is followed by the dynamic characterization of the cantilever in still water, which has to be carried out previously to each test battery, for each sample tested. Table 1 presents average values of natural frequencies, obtained through standard (FFT) spectral analysis, from standard decaying tests in still water. The experimental results are compared with design values, obtained analytically and numerically. Decaying sampling frequency was set at 200Hz.

Table 1. Natural frequencies average values obtained in still water from decaying experiments compared with analytical and numerical values.

MODEL	ANALYTICAL			NUMERICAL			AS BUILT			RATIO DIVERSION
width x tickness	fx1 (Hz)	fy1 (Hz)	fx1 / fy1	fx1 (Hz)	fy1 (Hz)	fx1 / fy1	fx1 (Hz)	fy1 (Hz)	fx1 / fy1	"Analytic" x "As built"
2 x 2	2.357	2.355	1.001	2.360	2.36	1.000	2.050	2.030	1.010	0.9%
2 x 1	1.687	0.857	1.968	1.689	0.863	1.957	1.610	0.827	1.947	1.10%
3 x 1	3.074	1.037	2.964	3.073	1.043	2.946	2.760	1.010	2.733	7.81%
4 x 1	4.690	1.187	3.951	4.705	1.193	3.943	4.261	1.173	3.633	8.06%

Three different test batteries were planned, aiming at mitigating any assembly bias (see Tab. 2): (1) cantilever and anchor structure submerged and decentralized; (2) cantilever submerged and anchor lined-up with the water line but out of center with respect to the water channel width; (3) cantilever submerged, anchor lined up in the water line and centralized with respect to the water channel width.

Three runs composed each test battery. In each run, two conditions were taken, in continuously ascending and descending speeds. For the 2mm x 2mm flexible cantilever, the maximum reduced velocity (based on the first natural frequency, such that $U^*=U/f_{y1}D$) was set to U^*=15, such that the drag force acting would not overwhelm the aluminum strip yield stress at the anchor. The remaining models were tested up to a reduced velocity U^*=22. The channel speed was gradually increased or decreased, allowing an acquisition time of at least 100 crosswise oscillations after each control action. In this case, sampling frequency was set to 75Hz. Such a strategy resulted in very slow variations of the flow speed, in an almost linear faction with respect to time, as exemplified in Fig. 7.

Table 2. Test Matrix. I: increasing; D: decreasing

Test Battery 1	Test Battery 2	Test Battery 3	Model Dimensions (mm)	Run	Flow Speed	U (m/s) range	Re range	U* range
(1) anchor structure *submerged* and *out of center* with respect to the circulating water channel	(2) anchor structure *lined up with water line* and *out of center* with respect to the circulating water channel	**(3)** anchor structure *lined up with water line* and *centered* with respect to the circulating water channel	2x2	1	I	0.014 - 0.316	140 - 3150	0-15
					D	0.316 - 0.014	3150 - 140	15-0
				2	I	0.014 - 0.316	140 - 3150	0-15
					D	0.316 - 0.014	3150 - 140	15-0
				3	I	0.014 - 0.316	140 - 3150	0-15
					D	0.316 - 0.014	3150 - 140	15-0
			2x1	1	I	0.014 - 0.182	140 - 1814	0-22
					D	0.182 - 0.014	1814 - 140	22-0
				2	I	0.014 - 0.182	140 - 1814	0-22
					D	0.182 - 0.014	1814 - 140	22-0
				3	I	0.014 - 0.182	140 - 1814	0-22
					D	0.182 - 0.014	1814 - 140	22-0
			3x1	1	I	0.014 - 0.225	140 - 2243	0-22
					D	0.225 - 0.014	2243 - 140	22-0
				2	I	0.014 - 0.225	140 - 2243	0-22
					D	0.225 - 0.014	2243 - 140	22-0
				3	I	0.014 - 0.225	140 - 2243	0-22
					D	0.225 - 0.014	2243 - 140	22-0
			4x1	**1**	**I**	0.014 - 0.258	140 - 2572	0-22
					D	0.258 - 0.014	2572 - 140	22-0
				2	I	0.014 - 0.258	140 - 2572	0-22
					D	0.258 - 0.014	2572 - 140	22-0
				3	I	0.014 - 0.258	140 - 2572	0-22
					D	0.258 - 0.014	2572 - 140	22-0

4. EXPERIMENTAL ANALYSIS METHODOLOGY: A RECURSIVE APPLICATION OF THE HILBERT-HUANG TRANSFORM (HHT)

The ultimate focus of this experimental investigation is the construction of charts presenting significant vibration amplitude and dominant frequencies responses, corresponding to distinct vibration modes and obtained as function of reduced velocity, parameterized according to the frequency ratio. However, as a novel analysis methodology had to be developed to deal with the experimental procedure strategy, the full set of data will be analyzed afterwards, once such a methodology has been consolidated. Preliminarily, in the present paper, the analyzed data is thus restricted to the 4x1 mm model, focusing on the temporal series of the tip cartesian coordinates, obtained from just one run, in one battery test. The chosen run is marked in bold red in Tab 2.

In fact, the displacement signals experimentally obtained, revealed a non-stationary behavior, not typical of common VIV.; see Fig. 7. Moreover, the adopted water channel control strategy, by continuously decreasing/increasing the flow speed, if, on one hand, shortens the whole experiment duration, on the other turns standard analysis procedures - by isolating segments according to speed ranges - much harder to be applied. A non-standard time-domain analysis procedure is more appropriate, as those based on the HHT – Hilbert Huang Transform, Huang *et al* (1998); see Pesce *et al* (2006), for the pioneering application to VIV analysis. Besides the revealed non-stationarity, large mean deflections have been observed in the stream and cross wise directions. Both increase quadratically with the flow speed. The stream wise deflection is due to drag forces. The cross wise deflection is directed to one of the sides of the channel and is possibly provoked by a non-symmetric flow speed profile with respect to the central-longitudinal plane, caused by the arrangement of the underwater cameras placed downstream. These trends are exemplified in Fig. 7, through the x and y-coordinates time series measured at the tip of the 4x1 model and have to be removed from the original signal, leaving dynamic oscillations only.

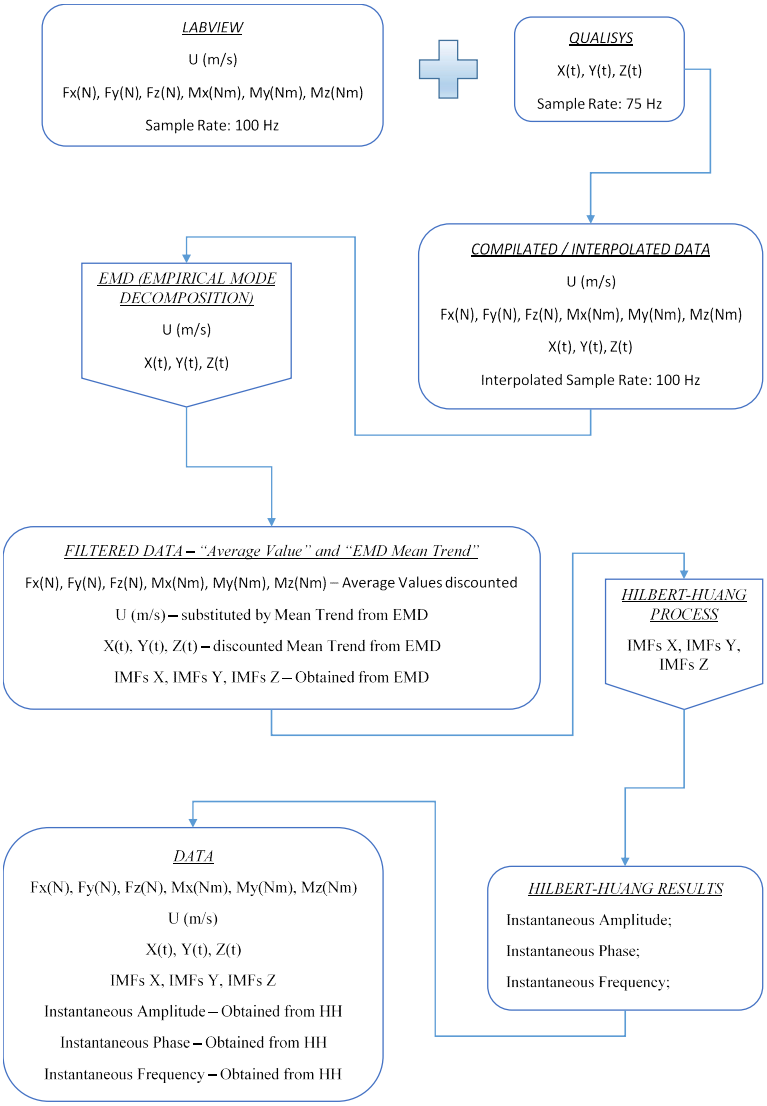

Figure 6. Experimental analysis methodology.

A novel analysis methodology, based on a recursive use of the Empirical Mode Decomposition (EMD) technique, which is the first step of the HHT, has then been implemented for this purpose. In fact, the EMD sifting process is a powerful filtering tool, enabling to separate the dynamic part, with null time average, from the main slowly varying trend of a signal. The EMD procedure decomposes the original time signal in *n-1 intrinsic mode functions* (IMFs), the dynamic ones, completed by a lasting and slowly varying residual one, which is called the *trend function*. The trend function gives the instantaneous average value of the signal. In the present case, the trend is the instantaneous slowly-varying bending, not furtherly considered in the dynamic analysis. Note that IMFs and the trend signal are functions of

time. As the flow speed is also a function of time, the IMFs and trend function can be given as functions of the reduced velocity.

Subsequently to the EMD, the Hilbert-Transform is applied to the set of IMFs, such as to allow the amplitude envelope and phase of each IMF to be determined, also as functions of the reduced velocity. The derivatives of the respective phase function, with respect to time, give then the instantaneous frequencies corresponding to each IMF. The amplitude envelope produces the respective instantaneous vibration amplitude. Notice that, usually, the first two or three IMFs contain almost the whole dynamic power embedded in the original signal.

An overview on the analysis methodology, at the stage developed up to this moment, is described in Fig. 6. It should be mentioned that such a recursive strategy is, in fact, a novel analysis methodology. As already mentioned, just a few examples of analysis will be shown in this paper. This is done in the next section. Deeper analyses are left for further work. It is the intent of the authors to apply the recursive HHT methodology to the signals emerged from a Galerkin decomposition in space, along the cantilever spam, such that each vibrating mode may be analyzed in the time domain.

5. PREMILINARY RESULTS

A few examples have been selected to illustrate the application of the experimental analysis methodology. A particular ascending speed run with the 4x1 model was taken. The chosen run is highlighted in Tab. 2, in bold red.

Figure 7 shows the flow speed and tip displacement coordinates in both directions. The original signals are shown in blue. Signal trends are presented in red. The trend in the stream wise direction is the more noticeable one, as it is caused by drag loading.

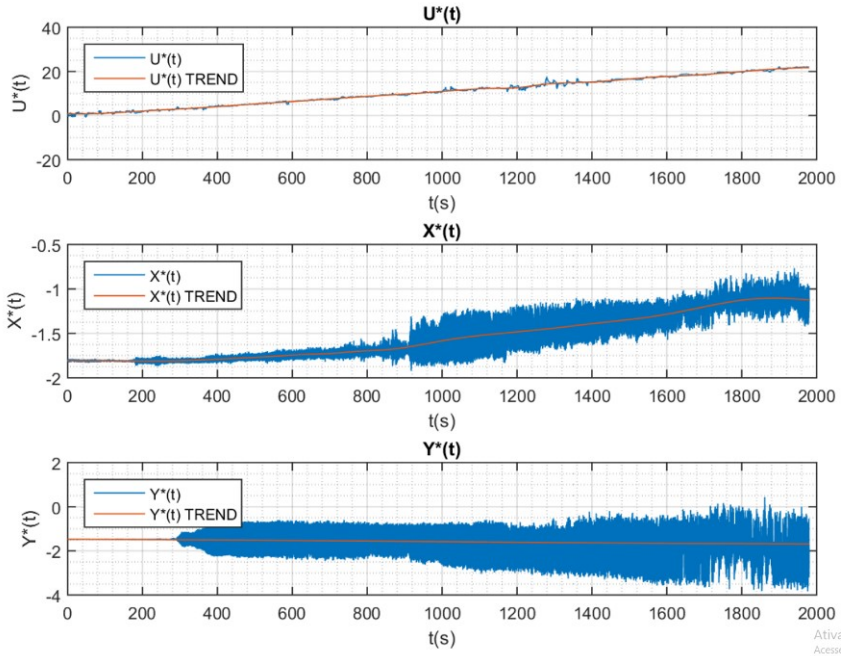

Figure 7. Top: Flow speed variation; Center and Bottom: 4x1 (mm) model tip (*x,y*) deflection. Original time series in blue and trends in red.

The cartesian coordinates of the 4x1 cantilever tip are shown again in Fig. 8, however as functions of the reduced velocity. After EMD is applied, removing the respective trends, the first three corresponding IMFs (Intrinsic Mode Functions) are shown in the three graphs below. The traces in blue correspond to the IMFs, whereas those in red are their instantaneous amplitudes (envelopes). Notice that the energy contained in the oscillating part of the original signal alternates between IMF 1 and 2, complemented by the content of IMF 3.

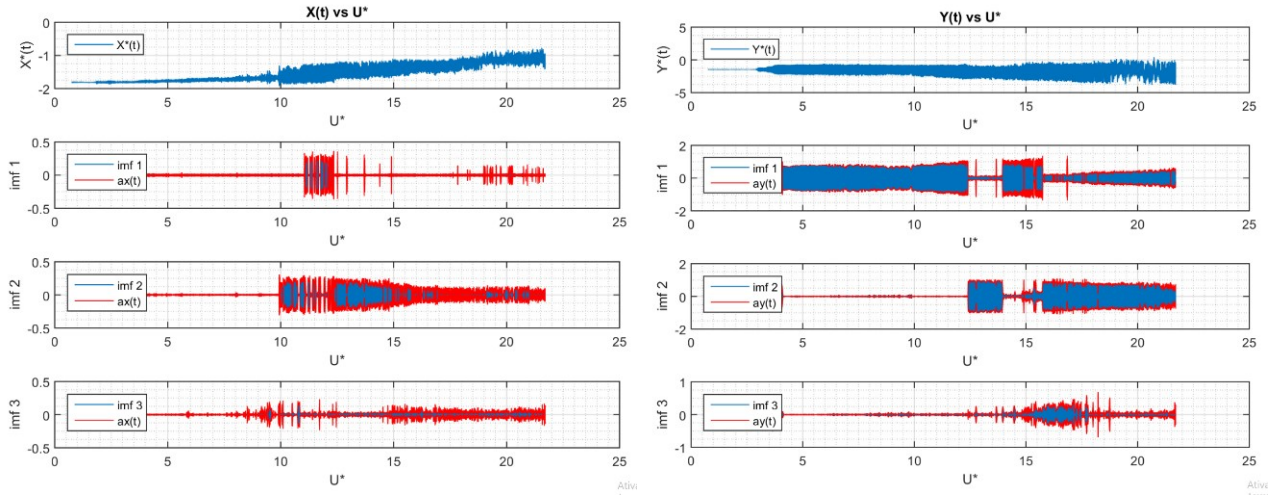

Figure 8. Model tip cartesian (X,Y) coordinates as function of reduced velocity. Top: original time series (in blue); Below: first three IMFs in blue; corresponding instantaneous amplitude (envelope) in red.

Figure 9 shows the envelopes, in the stream and cross wise directions, for the first three IMFs, replotted on the same graph, as function of the reduced velocity.

On the left, the stream wise instantaneous vibrating amplitude corresponding to IMF 1 and 2 (blue and red) may be roughly seen completing each other. A first and very small stream wise lock-in peak (A_x* ~ 0.05) can be noticed in IMF 1, at small reduced velocities, close to U*~2.5. Then a relatively large vibration amplitude can be seen starting at U*~10, peaking at U*~12 and decreasing to relatively small values for higher reduced velocities.

On the right, a cross wise instantaneous vibrating amplitude response may be also roughly perceived, mostly from IMFs 1 and 2 (blue and red). A first mode lock-in initiates with a sharp increase, starting at U*~ 3.5, in a classic cross wise VIV, developing from the initial to the upper amplitude branch. In pure flexible cylinder VIV, the lock-in range extends up to U*~12, see Fig. 1, with the upper branch peaking at U*~ 6, followed by a lower branch which ends at U*~ 12 and leaves buffeting as a ground vibration from there on. In the present experiment however, such a classic behavior is not observed. Indeed, after a maximum amplitude around A_y*~0.8 at U*~ 6, followed by a small decrease, a high amplitude branch starts developing at U*~10, forming the so-called high-energy mode branch (HEMB. The HEBM peaks at U*~ 16, with an amplitude value A_y*~1.0, extending over a large reduced velocity range, up to the maximum reduced velocity tested, U*~22, where an appreciable amplitude of order 0.8 can still be observed.

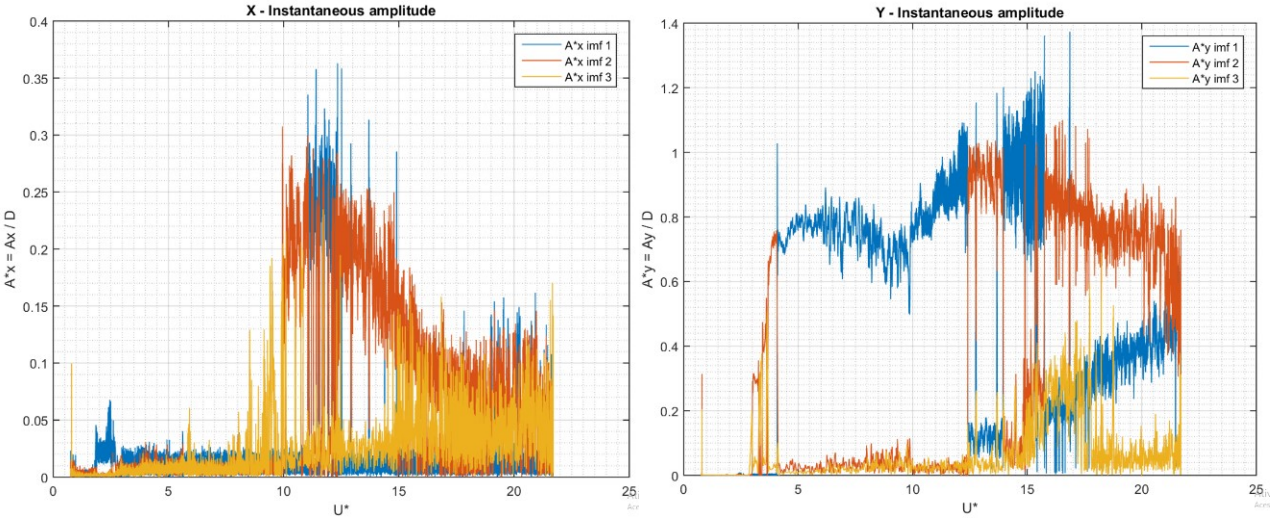

Figure 9. First three IMFs instantaneous amplitude in both directions as functions of reduced velocity.

Note that the HEMB strongly couples stream and cross wise vibrations for U*>10, showing a decreasing amplitude, after this point. Recall that only the 4x1 model has been exemplified. Data corresponding to the other three cylinders tested are still under analysis. However it can be already anticipated that the same kind of behavior has been observed.

6. CONCLUSIONS

Motivated by further understanding the VIV 'high speed mode branch', found experimentally by Fujarra, *et al.*, 2001, in cantilevered flexible cylinders with orthotropic bending stiffness, an experimental campaign has been carried out in a recirculating water channel. This campaign comprised experiments with four cantilevered cylinders presenting distinct natural frequencies ratios in the stream and the cross wise directions. Such a fluid-structure interaction vibrating phenomenon has been renamed as 'high energy mode branch' (HEMB), as it is characterized by large oscillating amplitudes extending over a relatively wide range of reduced velocities, thus containing high frequencies and, subsequently, energy.

The design and manufacturing process of the flexible cylinders with orthotropic bending stiffness, as well as the test planning and the experimental set up were described. An underwater optical system was used to experimentally determine the elastic line, from displacements of distinct cross sections directly obtained by tracking reflective tapes attached along the cylinder.

By gradually varying the flow speed, experimental runs spanned a whole range of reduced velocities, generating a set of continuous and non-stationary signals, containing the cartesian coordinates of each target as functions of time. To cope with the signal analysis task, a novel analysis methodology, based on the Hilbert-Huang Transform (HHT), which uses the Empirical Mode Decomposition (EMD) technique, has then been introduced. Such a technique acts as a filtering tool, enabling to separate the dynamic part from the main slowly varying trend of a signal. The Hilbert Transform may be then applied to assess the instantaneous vibrating amplitude and dominant frequencies of intrinsic mode functions, which contain most of the signal energy. If applied recursively, such procedure provides good estimates of amplitude and frequency responses. The analysis methodology was then preliminarily tested, by chosen one specific run and analyzing the stream and cross wise displacements of the cantilever tip. The HEMB has then been observed.

Further work will combine the novel signal analysis procedure to Galerkin's projection techniques, generating instantaneous amplitudes and frequencies of vibrating modes as functions of time and reduced velocities.

7. ACKNOWLEDGMENTS

Authors are grateful to Prof. Dr. Gustavo R.S. Assi and MSc Murilo Cicolin, for enabling the use of the NDF water channel facilities and for helping during the experiments. Dr. Pedro Cardozo de Mello and Professor Kazuo Nishimoto, from TPN-USP are acknowledged for the use of the Qualisys® optical tracking system. A PPGEN – Graduate Program in Naval and Ocean Engineering, social demand CAPES MSc scholarship and two CNPq research grants, ns. 308990/2014-5 and 310595/2015-0, are acknowledged.

8. REFERENCES

Assi, G.R.S. (2005). Estudo experimental do efeito de interferência no escoamento ao redor de cilindros alinhados. MSc Dissertation (in Portuguese), Escola Politécnica, University of São Paulo.

Franzini, G.R; Gonçalves, R.T., Pesce, C.P., Fujarra, A.L.C., Mazzili, C.E.N., Meneghini, J.R., Mendes, P. (2015). Vortex-induced vibration experiments with a long semi-immersed flexible cylinder under tension modulation: Fourier transform and Hilbert-Huang spectral analyses. J. Braz. Soc. Mech. Sci. Eng., v. 37: 589-599.

Franzini, G.R; Pesce, C.P.; Gonçalves, R.T., Fujarra, A.L.C., Mendes, P. (2016). Experimental Investigations On Vortex-Induced Vibrations With A Long Flexible Cylinder. Part I: Modal Analysis With a Vertical Configuration. FIV 2016, Proceedings of the 11th International Conference on Flow Induced Vibration & Noise, The Hague, Holand, 2016.

Fujarra, A.L.C. (1997). Estudo em Modelo Reduzido de Tubo, Flexível e Liso, Submetido ao Fenômeno de Vibração Induzida Pela Vorticidade "Vortex Induced Vibration". MSc Dissertation (in Portuguese), Escola Politécnica, University of São Paulo.

Fujarra, A.L.C. (2002). Estudos Experimentais e Analiticos das Vibrações Induzidas Pela Emissão de Vórtices Em Cilindros Flexíveis e Rígidos. PhD Thesis, (in Portuguese), Escola Politécnica, University of São Paulo.

Fujarra, A.L.C., Pesce, C.P., Flemming, F., & Williamson, C.H.K. (2001). Vortex-Induced Vibration of a Flexible Cantilever. Journal of Fluids and Structures, v. 15: 651-658.

Huang, N.E., . Shen, Z., Long, S.R., Wu, M.C., Shih, H.H., Zheng, Q., Yen, N-C., Tung, C.C.,Liu, H.H. (1998), The Empirical Mode Decomposition and the Hilbert Spectrum for Non-linear and Non-stationary Time Series Analysis, Proc. R. Soc. Lond. A, v. 454: 903-995.

Pesce, C.P., Fujarra, AL.C. (2000). Vortex-Induced Vibrations and Jump Phenomenon: experiments with a clamped flexible cylinder in water. Int J. of Offshore and Polar Engineering, v. 10: 26-33.

Pesce, C.p., Fujarra, A.L.C. (2005). The "Super-Upper Branch" VIV Responde of Flexible Cylinders. 4th Conference on Bluff Wakes and Vortex-Induced Vibrations, Santorini, Greece, 2005.

Pesce, C.p., Fujarra, A.L.C., Kubota, L. (2006). The Hilbert-Huang Spectral Analysis Method Applied to VIV. Proceedings of the 25th International Conference on Offshore Mechanics and Arctic Engineering, OMAE2006-92119, v.4., pp. 551-561, Hamburg, Germany, 2006.

Salles, R., Pesce, C.P. (2017). Experimental assessments of the Added Mass of Flexible Cylinders in Water: the Role of Modal Shape Representation, DINAME2017, Proceedings of the XVII International Symposium on Dynamic Problems of Mechanics, São Sebastião, Brazil, 2017.

9. RESPONSIBILITY NOTICE

The authors are the only responsible for the printed material included in this paper.